Available online at www.sciencedirect.com

SCIENCE DIRECT

Nanomedicine: Nanotechnology, Biology, and Medicine 2 (2006) 1–7

nanomedicine

www.nanomedjournal.com

Basic Nanomedicine

Dynamics of GPI-anchored proteins on the surface of living cells

Anja Nohe, PhD,[a] Eleonora Keating, PhD,[b] Marc Fivaz, PhD,[c] F. Gisou van der Goot, PhD,[d] Nils O. Petersen, PhD[b,*]

[a]*Department of Chemical and Biological Engineering, Institute of Molecular Biophysics, University of Maine, Orono, Maine*
[b]*Department of Chemistry, University of Western Ontario, London, Ontario, Canada*
[c]*Department of Genetics and Microbiology, Centre Médicale Universitaire (C.M.U.), Geneva, Switzerland*
[d]*Department of Microbiology and Molecular Medicine, C.M.U., Geneva, Switzerland*

Received 15 September 2005; Accepted 10 October 2005

Abstract Rather than being distributed homogeneously on the cell surface, proteins are probably aggregated in clusters or in specific domains. Some of these domains (lipid rafts) have lipid compositions, which differ from their surrounding membrane. They have been implicated in cell signaling, cell adhesion, and cholesterol homeostasis. Estimates of their size vary from 40 to 350 nm in diameter depending on the study and cell type used. Rafts are enriched in glycosphingolipids and cholesterol and appear to be in a more ordered lipid phase. Although there is some knowledge of their function in cell signaling, less is known about their assembly and dynamics in cells at various temperatures. We use image correlation spectroscopy and dynamic image correlation spectroscopy to study the clustering and diffusion of glycosylphosphatidylinositol (GPI)-anchored proteins within the plasma membrane of living cells at various temperatures. We find that GPI-anchored proteins occur both as monomers and in clusters at the cell surface. The propensities to cluster as well as the diffusion coefficient of these clusters are strongly temperature dependent. At 37 °C the GPI-anchored proteins are highly dynamic with a lower state of clustering than at lower temperatures.

Key words: Image correlation spectroscopy; Flourescence; green flourescent protein (GFP); glycosylphosphatidylinositol (GPI); dynamic image cross correlation spectroscopy (DICS)

Lipid rafts are lipid microdomains with an estimated size between 40 and 350 nm. They are enriched in sphingolipids and cholesterol and play important roles in cell signaling, cell adhesion, and cholesterol homeostasis [1-6]. They have also been shown to be involved in the internalization of proteins on the cell surface [4,7-12]. The lipid composition of lipid rafts generates a more ordered lipid environment compared with the rest of the plasma membrane. This is due to the better packaging of long saturated acyl chains of the glycosphingolipids and cholesterol resulting in high melting temperature and resistance to solubilization in nonionic detergents at low temperatures. Glycosylphosphatidylinositol (GPI)-anchored proteins as well as trimeric and small GTPases, Src family kinases, lipid, messengers, and cytosolic signal transducers have been found in lipid rafts in vitro [13-19]. Most of the proteins are targeted to these domains by lipid modifications, such as GPI or acyl anchors, although some transmembrane proteins are palmitoylated. Recruitment of proteins in lipid rafts does not seem to depend on specific peptide motifs [18,20-22].

Although several proteins seem to be present in these microdomains, the dynamics and aggregation of the domains themselves are poorly understood. One important question is the protein's ability to laterally diffuse across cell membranes and how this is dependent on lipid rafts. As was shown in lipid bilayers, the lateral mobility of lipids in a liquid-ordered phase is slower than in a liquid-disordered phase [2,23-26]. Furthermore, current research suggests that proteins and lipids undergo constrained and/or slowed diffusion within rafts [27-29]. Moreover, raft proteins are stably associated for minutes with discrete domains, which themselves can diffuse across the cell surface [30]. The lateral diffusion of proteins is typically 10- to 100-fold

* Corresponding author.
E-mail address: nils.petersen@nrc.gc.ca (N.O. Petersen).

1549-9634/$ – see front matter © 2006 Published by Elsevier Inc.
doi:10.1016/j.nano.2005.10.013

slower in cell membranes than in model membrane systems, even for lipid-binding proteins such as cholera toxin B subunit [31].

Here we introduce image correlation spectroscopy (ICS) combined with dynamic image correlation spectroscopy (DICS) as tools to study the aggregation, diffusion, and reorganization of GPI-anchored protein domains at 37 °C, 19 °C (room temperature; RT), and 4 °C. As a model of the GPI-anchored protein we used a green fluorescent protein (GFP)-GPI fusion protein (see Methods; this construct contains the signal sequence of rabbit lactase phlorizin hydrolase (LPH), an N-glycosylation site thought to be important for proper targeting and the GPI attachment signal of lymphocyte function-associated antigen type 3 (LFA-3)).

Our data suggest that at 37 °C the GPI-anchored protein exists in at least two populations. The first is distributed homogeneously over the membrane, whereas the second is aggregated in clusters. The homogeneously distributed population diffuses too rapidly to be measured by DICS (3.9×10^{-8} cm^2 s^{-1} [30]), whereas the diffusion coefficient for the clusters is much smaller ($\sim 6 \times 10^{-12}$ cm^2 s^{-1}). Treatment with β-cyclodextrin, a drug that extracts cholesterol from membranes and therefore affects lipid rafts, at 37 °C results in more numerous but smaller clusters that have a larger diffusion coefficient. Reducing the temperature from 37 °C to 19 °C leads to a decrease in the homogeneously distributed population yielding more and larger clusters that have a reduced mobility. Our results indicate that the GPI-anchored proteins are in domains that are very dynamic but sensitive to temperature.

Materials and methods

Materials

The cell line COS-7 (CRL 1651) was purchased from American Type Culture Collection (ATCC, Manassas, VA). The GFP-GL-GPI is a fusion protein containing the signal sequence of rabbit LPH [30], an N-glycosylation site thought to be important for proper targeting, and the GPI attachment signal of LFA-3, and was provided by Patrick Keller (MPI, Dresden, Germany).

Transfection of COS-7

COS-7 cells were grown in Dulbecco's modified Eagle's medium (DMEM) supplemented with 10% fetal bovine serum (GibcoBRL, Burlington, ON, Canada) and transfected by Fugene (Roche, Mississauga, ON, Canada) according to the manufacturer's protocol. Transfections were done on cells grown in 35-mm-diameter dishes using 1 μg of DNA per plasmid construct.

Treatment of transfected COS-7 cells with 2-hydroxypropyl-β-cyclodextrin

The transfected COS-7 cells were incubated 1 hour before the image collection with 10 μg/mL 2-hydroxypropyl-β-cyclodextrin (Sigma, St. Louis, MO) dissolved in DMEM at 37 °C. The cyclodextrin was present throughout the subsequent confocal measurements.

Confocal microscopy

The transfected COS-7 cells were placed on a 22-mm-diameter coverslip that was inserted into a temperature stage. The temperature stage was regulated at 37 °C, 19 °C (RT), or 4 °C.

Transfected cells were visualized using a Biorad MRC 600 confocal microscope equipped with an Ar/Kr mixed-gas laser and using the appropriate filter sets for dual-fluorophore imaging. Cells expressing the protein were selected under mercury lamp illumination using a 60× (1.4 numerical aperture) objective and an inverted Nikon microscope. An area on the cell at a distance from the nucleus was enlarged and visualized. For measuring GFP fluorescence the filter wheel was set for 488 nm laser excitation, and neutral density filters were used to attenuate the laser to 1% laser power. One scan was accumulated on photomultiplier tube 2 (PMT2) in the photon counting mode (to ensure linear scaling of the intensity). The PMT was set with the black level at 6.0 on the vernier scale, and the gain was set at 10. Every 10 seconds a high-magnification image was recorded. After the collection of each set of 50 images, images were collected using identical settings but with the shutter to the sample closed, to obtain a measure of the dark current for each PMT. A total of six data sets were collected on different cells in different samples at each temperature.

Image correlation spectroscopy

ICS and DICS are two techniques that are used to study the distribution and localization of the GPI-anchored protein. ICS involves autocorrelation analysis of the intensity fluctuations within confocal images collected in this case from transfected cells that contain GFP-tagged GPI-anchored proteins.

Let the fluorescent intensity in a pixel located at position x,y in the image be i(x,y); then the corresponding normalized fluorescence intensity fluctuation, δi(x,y), is given by:

$$\delta i(x,y) = \frac{i(x,y) - <i(x,y)>}{<i(x,y)>} \quad (1)$$

The normalized spatial autocorrelation function, g($\xi\eta$), is then given by:

$$g(\xi,\eta), = <\delta i(x,y)\delta i(x+\xi, y+\eta)> \quad (2)$$

where the angular brackets indicate the average over all spatial coordinates and ξ and η are position lag coordinates for the x- and y-axes. It is known that the limit of the autocorrelation function as ξ and η approach zero, g(0,0), is equal to the variance of the normalized intensity fluctuations.

It is also known that for homogeneous, noninteracting species, where the intensity is a true representation of the

concentration, the variance of the normalized intensity fluctuations is equal to the variance of the concentration fluctuations, which in turn is equal to the inverse of the number of particles in the observation area, N_p [32].

$$g(0,0) = var(\delta i(x,y)) = var(\delta c(x,y)) = \frac{1}{\overline{N}_p} \tag{3}$$

Once the g(0,0) is known, an important parameter, called the cluster density (CD) can be calculated. The CD value gives the average number of receptor clusters per unit area.

$$CD = \frac{1}{g(0,0)w^2\pi} = \frac{\overline{N}_p}{\pi w^2} \tag{4}$$

Dynamic image correlation spectroscopy

DICS is an extension of ICS. In DICS, a time-dependent cross-correlation function is generated by calculating the mean fluorescence intensity fluctuations arising from images collected at different times but on the same area of the same cell labeled for the same protein. If the intensity of the protein at time t is i(t), and the intensity of the protein after a time τ is i(x + χ, y + ξ, t + τ), then the normalized, time-dependent cross-correlation function $g_{iit}(\chi,\xi,\tau)$ can be calculated as:

$$g_{iit}(\chi,\xi;\tau) = \frac{\left\langle \left(i(x,y;t) - \langle i(x,y;t)\rangle\right)\left(i(x+\chi,y+\xi;t+\tau) - \langle i(x,y;t)\rangle\right)\right\rangle}{\langle i(x,y;t)\rangle^2} \tag{5}$$

From this the normalized amplitude of the time-dependent cross-correlation function, $g_x(0,0,\tau)$ can be calculated as:

$$g_x(0,0,\tau) = \lim_{\chi\to 0,\xi\to 0} \frac{\left\langle \left(i(x,y;t) - \langle i(x,y;t)\rangle\right)\left(i(x+\chi,y+\xi;t+\tau) - \langle i(x,y;t)\rangle\right)\right\rangle}{\langle i(x,y;t)\rangle^2} = \frac{1}{\overline{N}_\mu} F(\tau) \tag{6}$$

where $\overline{N}_\mu$ is an approximate estimate of the average number of clusters in the observation area. $F(\tau)$ is a function that measures the rate at which correlation of the image disappears. The cross-correlation function represented by Eq. (6) may be thought of as an averaged fluorescence correlation function for the ensemble of all collection volumes in the image.

With an analogy to single-point fluorescence correlation spectroscopy measurements and restricting to the case of two-dimensional diffusion, $F(\tau)$ can be approximated by:

$$F(\tau) = \frac{1}{1 + \tau/\tau_d} \tag{7}$$

Calculations of fluctuations of the cluster density in a 100-second time window

To obtain a sense of the variation of the number of clusters on the surface with time, we calculate a parameter P(100) as a measure of the relative variations in the CD at a 100-second time scale. We define P(100) as:

$$P(100) = \frac{var(CD_{100}(n))}{mean\left(\overline{CD}_{100}(n)\right)} * 100 \tag{9}$$

where $CD_{100}(n) = \sum_{j=0}^{9} CD(n+j)/10$ represents the sliding average of the CD over a sequence of 10 images (100 seconds). P(100) is zero if there is no variation in the state of aggregation with time (ie, all clusters remain the same size but they move). P(100) is 100% if the average cluster size varied by a random process following Poisson statistics (var = mean, that is, the variation in the number of clusters is random at the 100-second time scale). P(100) is less than 100% if the random fluctuations are at a much different time scale.

Statistics

Standard error of the mean (SEM) values were calculated from the raw data at the 95% confidence level.

Results

Diffusion of the GPI-anchored proteins on the cell surface

To analyze the dynamics of GPI-anchored proteins on the cell membrane, we transfected COS-7 cells with the GFP-GPI fusion protein. After 48 hours the transfected cells were placed in a temperature stage, and 50 high-magnification images were taken at the 10-second interval of the GPI-GFP at the plasma with a confocal microscope. Using this approach we detect only the movement of the bigger clusters of the protein, which move slower on the plasma membrane; the diffusion of individual proteins, which are much faster, is not measured. From the images obtained, the amplitude of the normalized time-dependent cross-correlation function $g_x(0,0,\tau)$ was calculated and plotted as a function of the delay time (Figure 1). Fitting the curve shown in Figure 1 to a three-parameter hyperbolic decay of the form:

$$g_x(0,0,\tau) = g_x(0,0,0) + \frac{1}{\overline{N}_\mu} * \frac{1}{1 + \tau/\tau_d} \tag{10}$$

the diffusion time τ_d can be obtained. Once τ_d is known the diffusion coefficient D can be calculated according to:

$$D = \frac{w^2}{4*\tau_d} \tag{11}$$

The diffusion coefficients obtained for the GPI-anchored protein at 37 °C, RT, and 4 °C are shown in Figure 2. At 37 °C the diffusion coefficient (6×10^{-12} cm^2 s^{-1}), is approximately fivefold greater than the diffusion coefficient at RT (give value to quantify). The movement of the clusters at 4 °C was very slow, roughly 100 times slower than at 37 °C, but in general it was not possible to fit the cross-correlation functions well.

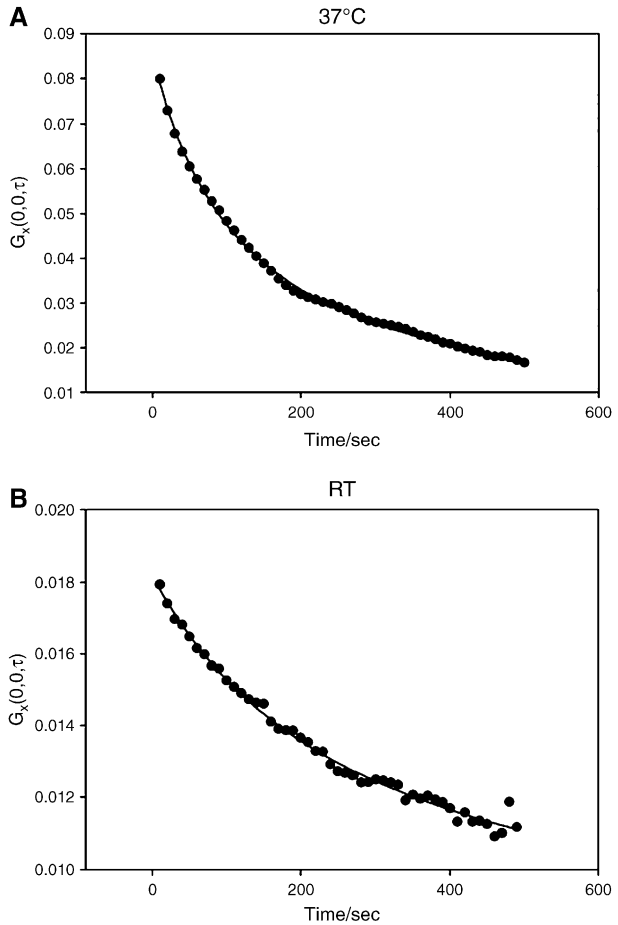

Fig 1. Plot of the cross-correlation fit as a function of difference in time between images. Result at 37 °C (**A**) and at room temperature (**B**).The solid lines represent the best fit. The intercept on the y-axis is used to calculate average cluster density (CD_a). The decay fits a slow diffusion process and approaches zero for long times.

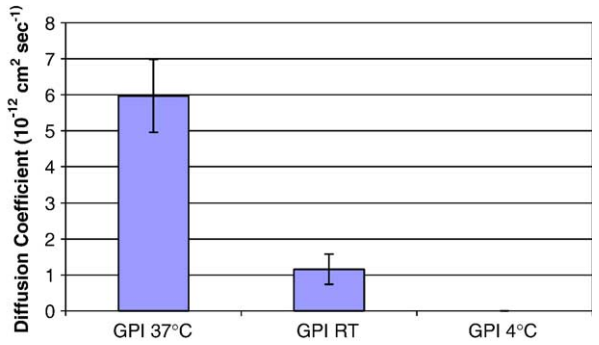

Fig 2. Average diffusion coefficient for six separate experiments at each of the three temperatures. GPI-GFP diffuses about five times faster at 37 °C than at room temperature and about 100 times faster than at 4 °C.

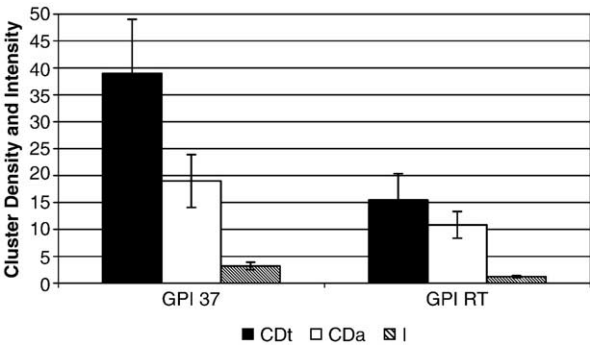

Fig 3. COS7 cells were transfected with GPI-GFP. 48h after the transfection cells 50 high magnification images delayed with 10 s at 37 °C, RT were taken of 6 cells. The average total cluster density (CDt) of GPI-GFP was calculated using ICS. Extrapolating the time dependent amplitude of the cross correlation function also the Number of slow diffusing clusters CDa were calculated. At 37 °C the GPI-GFP exists as two populations, while at RT the fast moving population is decreased about a factor of 3.

Clustering of GPI-anchored proteins in living cells

To study the clustering of GFP-GPI, we calculated the number of clusters per unit area (CD) from each image. For a two-population system of monomers and oligomers it can be shown that the amplitude of the autocorrelation function g(0,0) can be approximated by the following:

$$g(0,0) = \frac{1}{\overline{N}_m^2} * \left(\overline{N}_1 + \overline{N}_\mu * \mu^2\right) \tag{12}$$

where $\overline{N}_m$ is the average total number of GPI-anchored proteins, $\overline{N}_1$ is the average number of molecules present in the monomeric population, $\overline{N}_\mu$ is the average number of clusters, and μ is the mean number of molecules in the clusters. With $\overline{N}_m = \overline{N}_1 + \overline{N}_\mu * \mu$ the amplitude of the autocorrelation function is approximated by:

$$g(0,0) = \frac{1}{\overline{N}_m^2} * \left(N_m - \overline{N}_\mu * \mu + \overline{N}_\mu * \mu^2\right) \tag{13}$$

We can calculate the number of clusters, $\overline{N}_\mu$ by extrapolation of the time-dependent amplitude of the cross-correlation function (see Figure 2). We can calculate the number of molecules present in each of the two populations, if we can independently estimate either N_m or μ. We can estimate the average cluster density of the moving aggregates (CD_a). In Figure 3, CD_a is compared to the mean cluster density (CD_t) calculated from all autocorrelation functions. The difference between CD_t and CD_a reflects the relative amount of the two populations in the system, the clusters and the monomeric population, respectively. It is interesting to note that at RT, CD_a is not significantly different from the CD of the whole populations, suggesting that only a small number of the proteins are present in the monomer population; that is, most of the proteins are in clusters (see Figure 4). As a result of the very slow diffusion of the clusters at 4 °C, the CD_a cannot be reliably estimated.

As these data indicate, at 37 °C the GPI-anchored protein exists as two populations. Cooling the cells to RT leads to a decrease of the monomeric population $\overline{N}_1$. Most proteins are now present in clusters $\overline{N}_\mu$ At the same time the total

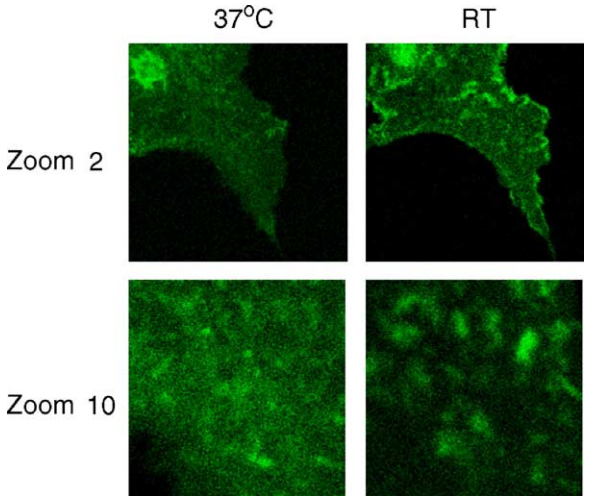

Fig 4. GPI-GFP exists as 2 populations at 37 °C on the cell surface. Changes in the temperature to RT lead to a decrease in the homogenous population. COS7 cells were transfected with GPI-GFP. 48 h after transfection a Zoom 2 and a Zoom 10 image of the same cell were taken at 37 °C and RT. The larger sizes of the fluorescent objects and the weaker background fluorescence in the RT image are consistent with the absence of monomers at this temperature.

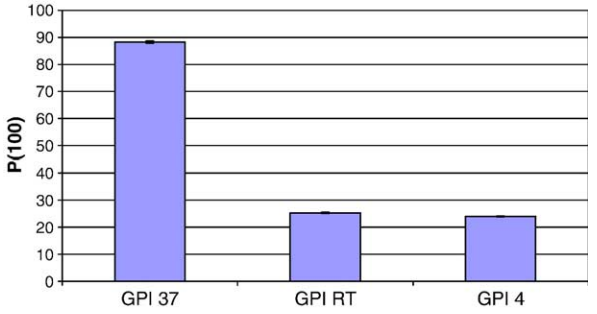

Fig 5. The P(100) which represents the aggregation and dispersion dynamic of the GPI-GFP- clusters were calculated at 37 °C, RT and 4 °C. Cooling the cells to RT or 4 °C leads to an decrease in the clustering and dispersion of the clustered domains of about an factor of 2.

average number of molecules expressed on the cell surface is smaller by a factor of approximately 3 compared with that at 37 °C, because the average fluorescence intensity is lower by about a factor of 3. This difference may arise from the different expression levels in transfected COS-7 cells at the two temperatures.

Dynamics of the aggregation and dispersion of the GPI-anchored protein

To examine the dynamics of the GPI-anchored protein in more detail we analyzed the changes in the cluster density during a period of time. For this we examined the fluctuations during 100 seconds expressed as the parameter P(100). These results are summarized in Figure 5. The fluctuations in CD are approximately sixfold higher at 37 °C than at RT or 4 °C. This indicates that at 37 °C the aggregation and dispersion of the GPI-anchored protein clusters is more dynamic at the 100-second time scale. This

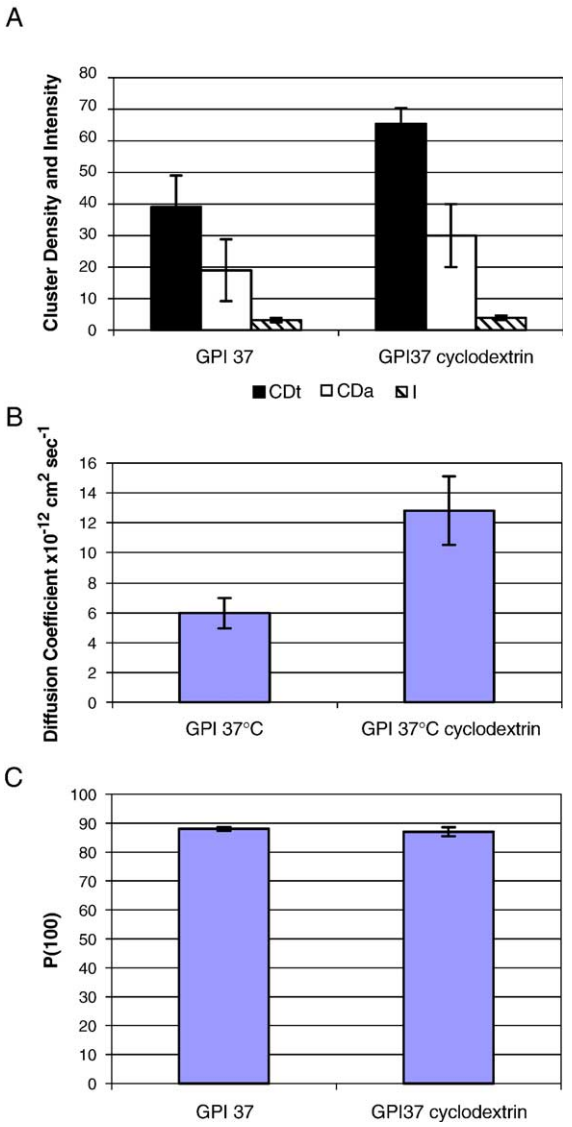

Fig 6. 48 h after the transfection with GFP-GPI COS7 cells were incubated or not incubated for 1 h with cyclodextrin at 37 °C. 50 high magnification images delayed by 10 s were taken and the Diffusion coefficient, the CD and the P(100) was calculated as described in the text. The treatment results in an increase in the Diffusion coefficient and the CD. The P(100) is not significantly changed.

variation of the CD value is probably due to changes in the numbers of clusters as protein monomers associate to form clusters or dissociate to dissolve clusters. At RT most proteins are in clusters already, and this shift in population is not possible, as seen by the lower variations in the CD values during a period of time.

Treatment of cells with cyclodextrin leads to a dispersion of the GPI-anchored proteins

2-Hydroxypropyl-β-cyclodextrin is known to extract cholesterol from the plasma membrane and thereby affects raft structure, function, and dynamics [references]. Our data indicate that the treatment with β-cyclodextrin for 1 hour at

37 °C does not alter the total number of GPI-anchored proteins on the plasma membrane because the fluorescent intensity is not significantly changed. However cyclodextrin leads to a dispersion of the GPI-anchored clusters, because both the average number of clusters CD_a and CD_t increase (Figure 6, *A*). That the treatment did not significantly affect the ratio of the two populations' $\overline{N}_\mu/\overline{N}_1$, implies there are more numerous but smaller clusters following the cyclodextrin treatment. Importantly, cyclodextrin treatment does not lead to a complete monomerization of GFP-GPI, presumably explaining why GPI-anchored proteins still associate with detergent-resistant membranes after cyclodextrin treatment of cells [33]. The treatment also affects the diffusion of the clusters, leading to an approximately twofold increase in the diffusion coefficient (Figure 6, *B*). The value of P(100) was not affected (Figure 6, *C*).

These results indicate that the treatment with β-cyclodextrin affects only the aggregation of the GPI-anchored protein clusters and the diffusion, but does not change the dynamics of the assembling and disassembling of the GPI-anchored proteins.

Discussion

Our data indicate that diffusion, aggregation, and assembly of GPI-anchored protein clusters on the cell surface are dynamic and highly temperature-dependent processes. At physiological temperatures, the proteins exist in two populations: monomers and clusters. The former diffuse rapidly (3.9×10^{-12} cm^2 s^{-1}), whereas the latter diffuse very slowly (6×10^{-12} cm^2 s^{-1}), yet there is rapid exchange between the two populations. This rapid exchange leads to larger variations in the average number of clusters as a function of time. The slower moving clusters are probably lipid rafts, because cholesterol removal by cyclodextrin leads to the dispersion of more but smaller clusters that move more rapidly. This cyclodextrin sensitivity is consistent with the effect of cyclodextrin on lipid rafts. Our observation that the GPI-anchored proteins are still in clusters is consistent with the GPI-anchored proteins being observed in raft fractions even when cyclodextrin is present. As the temperature is lowered from 37 °C to RT and then to 4 °C, the mobility of the clusters decreases to virtual immobility. At the same time the number of monomers decreases dramatically, and at RT most of the GPI-anchored proteins expressed at the surface are in clusters that are large but fewer in number. This change in the distribution is consistent with lipid rafts being larger and hence more readily extracted as a detergent-resistant fraction, at low temperature.

References

[1] Simons K, Ikonen E. Functional rafts in cell membranes. Nature 1997;387(6633):569-72.
[2] Brown DA, London E. Functions of lipid rafts in biological membranes. Annu Rev Cell Dev Biol 1998;14:111-36.
[3] Jury EC, Kabouridis PS, Flores-Borja F, Mageed RA, Isenberg DA. Altered lipid raft-associated signaling and ganglioside expression in T lymphocytes from patients with systemic lupus erythematosus. J Clin Invest 2004;113(8):1176-87.
[4] Fielding CJ, Fielding PE. Cholesterol and caveolae: structural and functional relationships. Biochim Biophys Acta 2000;1529(1-3):210-22.
[5] Lucero HA, Robbins PW. Lipid rafts-protein association and the regulation of protein activity. Arch Biochem Biophys 2004;426(2):208-24.
[6] Garcia A, Cayla X, Fleischer A, Guergnon J, Alvarez-Franco Canas F, Rebollo MP, et al. Rafts: a simple way to control apoptosis by subcellular redistribution. Biochimie 2003;85(8):727-31.
[7] Janes PW, Ley SC, Magee AI, Kabouridis PS. The role of lipid rafts in T cell antigen receptor (TCR) signalling. Semin Immunol 2000;12(1):23-34.
[8] Kasahara K, Sanai Y. Functional roles of glycosphingolipids in signal transduction via lipid rafts. J Glycoconj 2000;17(3-4):153-62.
[9] Fielding CJ, Fielding PE. Membrane cholesterol and the regulation of signal transduction. Biochem Soc Trans 2004;32(Pt 1):65-9.
[10] Nichols BJ, Lippincott-Schwartz J. Endocytosis without clathrin coats. Trends Cell Biol 2001;11(10):406-12.
[11] Helms JB, Zurzolo C. Lipids as targeting signals: lipid rafts and intracellular trafficking. Traffic 2004;5(4):247-54.
[12] Nichols BJ, Kenworthy AK, Polishchuk RS, Lodge R, Roberts TH, Hirschberg K, et al. Rapid cycling of lipid raft markers between the cell surface and Golgi complex. J Cell Biol 2001;153(3):529-41.
[13] Kasahara K, Watanabe K, Kozutsumi Y, Oohira A, Yamamoto T, Sanai Y. Association of GPI-anchored protein TAG-1 with src-family kinase Lyn in lipid rafts of cerebellar granule cells. Neurochem Res 2002;27(7-8):823-9.
[14] Schraw W, Li Y, McClain MS, van der Goot FG, Cover TL. Association of *Helicobacter pylori* vacuolating toxin (VacA) with lipid rafts. J Biol Chem 2002;277(37):34642-50.
[15] Nichols B. Caveosomes and endocytosis of lipid rafts. J Cell Sci 2003;116(Pt 23):4707-14.
[16] Encinas M, Tansey MG, Tsui-Pierchala BA, Comella JX, Milbrandt J, Johnson Jr EM. c-Src is required for glial cell line-derived neurotrophic factor (GDNF) family ligand-mediated neuronal survival via a phosphatidylinositol-3 kinase (PI-3K)-dependent pathway. J Neurosci 2001;21(5):1464-72.
[17] Paladino S, Sarnataro D, Zurzolo C. Detergent-resistant membrane microdomains and apical sorting of GPI-anchored proteins in polarized epithelial cells. Int J Med Microbiol 2002;291(6-7):439-45.
[18] Hooper NM. Determination of glycosyl-phosphatidylinositol membrane protein anchorage. Proteomics 2001;1(6):748-55.
[19] Glebov OO, Nichols BJ. Distribution of lipid raft markers in live cells. Biochem Soc Trans 2004;32(Pt 5):673-5.
[20] Huang H, Ball JM, Billheimer JT, Schroeder F. Interaction of the N-terminus of sterol carrier protein 2 with membranes: role of membrane curvature. J Biochem 1999;344(Pt 2):593-603.
[21] Huang HW. Peptide-lipid interactions and mechanisms of antimicrobial peptides. Novartis Found Symp 1999;225:188-206.
[22] McIntosh TJ, Vidal A, Simon SA. Sorting of lipids and transmembrane peptides between detergent-soluble bilayers and detergent-resistant rafts. J Biophys 2003;85(3):1656-66.
[23] Brown DA, London E. Structure and function of sphingolipid- and cholesterol-rich membrane rafts. J Biol Chem 2000;275(23):17221-4.
[24] Korlach J, Schwille P, Webb WW, Feigenson GW. Characterization of lipid bilayer phases by confocal microscopy and fluorescence correlation spectroscopy. Proc Natl Acad Sci U S A 1999;96(15):8461-66.
[25] Dietrich C, Yang B, Fujiwara T, Kusumi A, Jacobson K. Relationship of lipid rafts to transient confinement zones detected by single particle tracking. J Biophys 2002;82(1 Pt 1):274-84.

[26] Kahya N, Scherfeld D, Bacia K, Poolman B, Schwille P. Probing lipid mobility of raft-exhibiting model membranes by fluorescence correlation spectroscopy. J Biol Chem 2003;278(30):28109-15.

[27] Jacobson K, Dietrich C. Looking at lipid rafts? Trends Cell Biol 1999; 9(3):87-91.

[28] Niv H, Gutman O, Kloog Y, Henis YI. Activated K-Ras and H-Ras display different interactions with saturable nonraft sites at the surface of live cells. J Cell Biol 2002;157(5):865-72.

[29] Rajendran L, Simons K. Lipid rafts and membrane dynamics. J Cell Sci 2005;118(Pt 6):1099-102.

[30] Pralle A, Keller P, Florin EL, Simons K, Horber JK. Sphingolipid-cholesterol rafts diffuse as small entities in the plasma membrane of mammalian cells. J Cell Biol 2000;148(5):997-1008.

[31] Bacia K, Majoul IV, Schwille P. Probing the endocytic pathway in live cells using dual-color fluorescence cross-correlation analysis. J Biophys 2002;83(2):1184-93.

[32] Wiseman PW, Hoddelius P, Petersen NO, Magnusson KE. Aggregation of PDGF-beta receptors in human skin fibroblasts: characterization by image correlation spectroscopy (ICS). FEBS Lett 1997;401(1):43-8.

[33] Abrami L, van Der Goot FG. Plasma membrane microdomains act as concentration platforms to facilitate intoxication by aerolysin. J Cell Biol 1999;147(1):175-84.